

Highly Luminescent Aniline and TiO₂ Composite: The Effect of Weight Ratio of Aniline and TiO₂

Byoung-Ju Kim¹⁾ · Eun-Hye Park²⁾ · Kwang-Sun Kang^{1)*}

¹⁾Department of New and Renewable Energy, Kyungil University, 50 Gamasilgil Hayangup Gyeongsan, Gyeongbuk 38-428, South Korea

²⁾Dasomdeul, 50 Gamasilgil Hayangup Gyeongsan, Gyeongbuk 38-428, South Korea

ABSTRACT: Strong deep ultraviolet emitting aniline and TiO₂ composite has been synthesized via hydrolysis and condensation reactions of titaniumisopropoxide (Ti(OPr)₄), aniline, and acetic anhydride. Three different weight ratios of aniline and Ti(OPr)₄ including 3:1 (TiO₂An-A), 2:1 (TiO₂An-B), and 1:1 (TiO₂An-C) were synthesized and characterized their optical properties. The FTIR spectra of the TiO₂An-A, -B, and -C showed the absorption intensities of the benzene ring stretching and bending vibrations, and benzene ring -CH stretching, bending, and deformation vibrations increased with the increase of the amount of aniline. The UV-visible absorption spectra showed that the UV region absorption was slightly increased with the increase of the amount of aniline. The photoluminescence (PL) intensities were exponentially increased with the increase the excitation wavelength from 307 to 317 nm, steadily increased from 300 to 313 nm and slowly increased from 302 to 308 nm for TiO₂An-A, -B, and -C, respectively and decreased thereafter. Therefore, the PL intensity is strongly dependent on the weight ratio of Ti(OPr)₄ and aniline.

Key words: TiO₂, Aniline, Composite, Photoluminescence

1. Introduction

Among the wide band gap oxide semiconductor materials, titanium dioxide (TiO₂) has been a great deal of research subject during the last decades due to its versatile nature for many application fields including efficient photocatalysts for waste water and gas purification, antireflection coatings, gas sensors (1), photoluminescence (PL) devices (2), energy efficient windows in solid state electrochromic devices (3), UV protection creams (4), and dye-sensitized solar cells (5). Composites of inorganic metal oxides and organic conducting polymers have been considerable interest in research and development of various application fields. For preparation of diverse TiO₂ and organic composites, sol-gel technique has many advantages including room temperature process, homogeneous composition, and control of composition. The unique advantage of sol-gel process is the control of the molecular precursor to the final product, which allows a better control of the whole process and the synthesis of diverse compositions for various applications. In TiO₂ sol-gel process, the metal alkoxide undergoes partial hydrolysis and polymerization, which gives titanium oxide

network.

Nano-/micro-structures of TiO₂ and conducting polymers, such as polyaniline (PAn), polypyrrole, polythiophene, poly(3,4-ethylenedioxythiophene), and their derivatives have been shown promising for application devices including sensors, biosensors, electrochromic devices, and rectification diodes. Among the conjugate polymers, PAn is one of the most important conducting polymers. It has been extensively investigated for various applications including corrosion protections (6), transparent conductors (7), sensors (8), battery applications (9), active electrodes (10), rechargeable batteries (11), and electrochromic displays (12). Although PAn has such a large variety of application fields, the major drawback of PAn is its insolubility in common solvents and its infusibility at elevated temperature, which makes poor processability. However, alkyl or amine substitution to the aromatic ring of the PAn chain largely enhances its solubility. Only a few investigations of mono- or di-substituted PAn have been reported. Conductive core-shell microparticles with thin PAn layers have been fabricated in the presence of colloidal core particles. We report the soluble PAn with TiO₂ and the characteristics of TiO₂ and PAn composite including FTIR spectra, UV-visible spectra, and photoluminescence spectra.

*Corresponding author: kkang@kiu.ac.kr

Received February 25, 2016; Revised February 29, 2016;

Accepted February 29, 2016

2. Experimental

2.1 Materials

Titaniumisopropoxide ($(\text{TiOPr})_4$, 97%), aniline (An, 99.5%), acetic anhydride (98%), and 2-propanol (99.5%) were purchased from Sigma Aldrich Co. Ltd. and used without further purification.

2.2 Synthesis

Schematic view of the synthetic process is depicted in Fig. 1. To the 100 ml of round bottom flask with a magnetic stirring bar, 12 g of 2-propanol, 3.0 g of $\text{Ti}(\text{OPr})_4$, and various amounts of aniline, such as 3.0 ($\text{TiO}_2\text{An-A}$), 2.0 ($\text{TiO}_2\text{An-B}$), and 1.0 g ($\text{TiO}_2\text{-An-C}$) were added to the flask. Finally, 1.2 ml of acetic anhydride was added to the flask and stirred at room temperature.

2.3 Measurements

The $\text{TiO}_2\text{An-A}$, -B, and -C was directly dropped, dried to a KBr plate, and obtained FTIR transmission spectrum using Nicolet iS5 FTIR spectrometer. Approximately 6 ml of methanol was added to a UV-visible cuvette, and added $\text{TiO}_2\text{An-A}$, -B, or -C to the cuvette, and obtained UV-visible spectra using Thermo Scientific Genesys 10S UV-visible spectrometer. PL spectra of $\text{TiO}_2\text{An-A}$, -B, or -C were obtained with Hitachi F-450 fluorescence spectrometer with the methanol- $\text{TiO}_2\text{An-A}$, -B, or -C TiO_2PAN solution.

3. Results and discussion

The composite of organic conducting polymer and inorganic oxide has discovered an extensive interest in research and

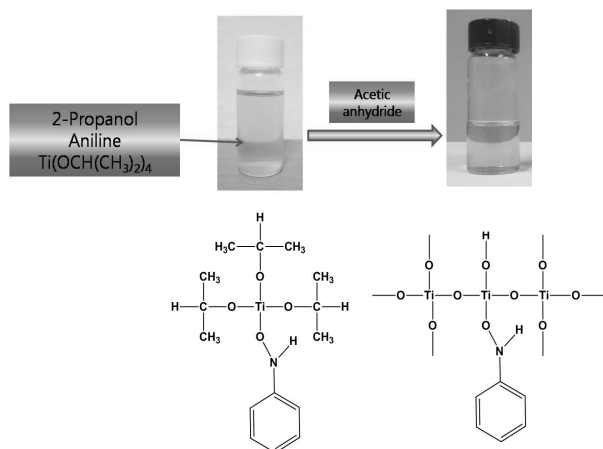


Fig. 1. Schematic representation of the synthetic process and possible chemical structures

development for many practical applications. The $\text{Ti}(\text{OPr})_4$ is very quickly hydrolyzed and precipitate from the solution with trace of water. Therefore, many researchers used $\text{Ti}(\text{OPr})_4$ stabilizer, such as diethanolamine, acetic acid, poly(ethylene glycol), 2-(2-methoxyethoxy)ethanol, and hydrochloric acid. Aniline was used as a $\text{Ti}(\text{OPr})_4$ stabilizer for the first time and was drastically increased the luminescence intensity by controlling the molar ratio of aniline and $\text{Ti}(\text{OPr})_4$. Schematic view of the

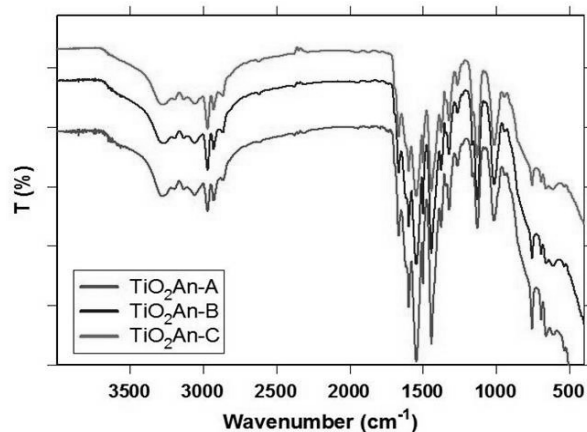


Fig. 2. FTIR spectra of (a) TiO_2An and (b) TiO_2PAN

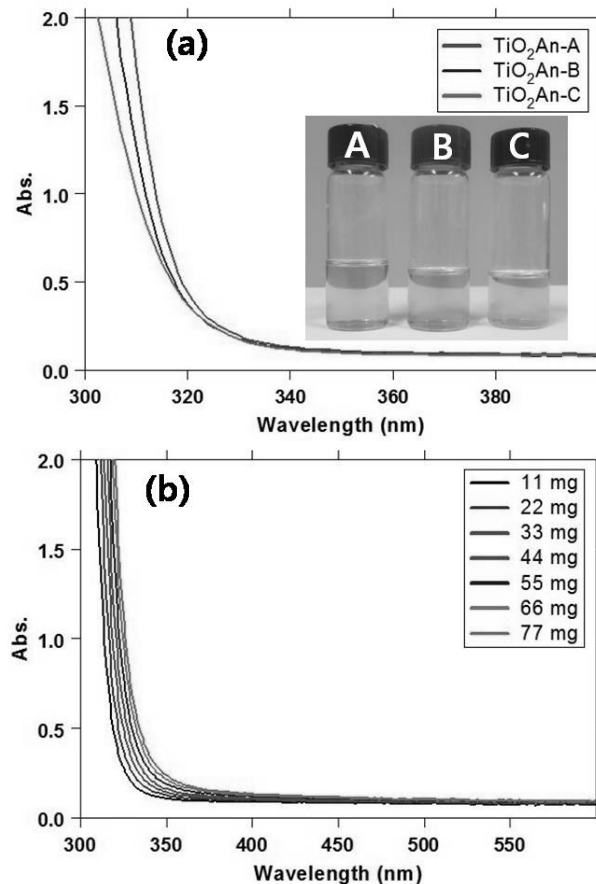


Fig. 3. UV-visible spectra of (a) TiO_2An and (b) TiO_2PAN

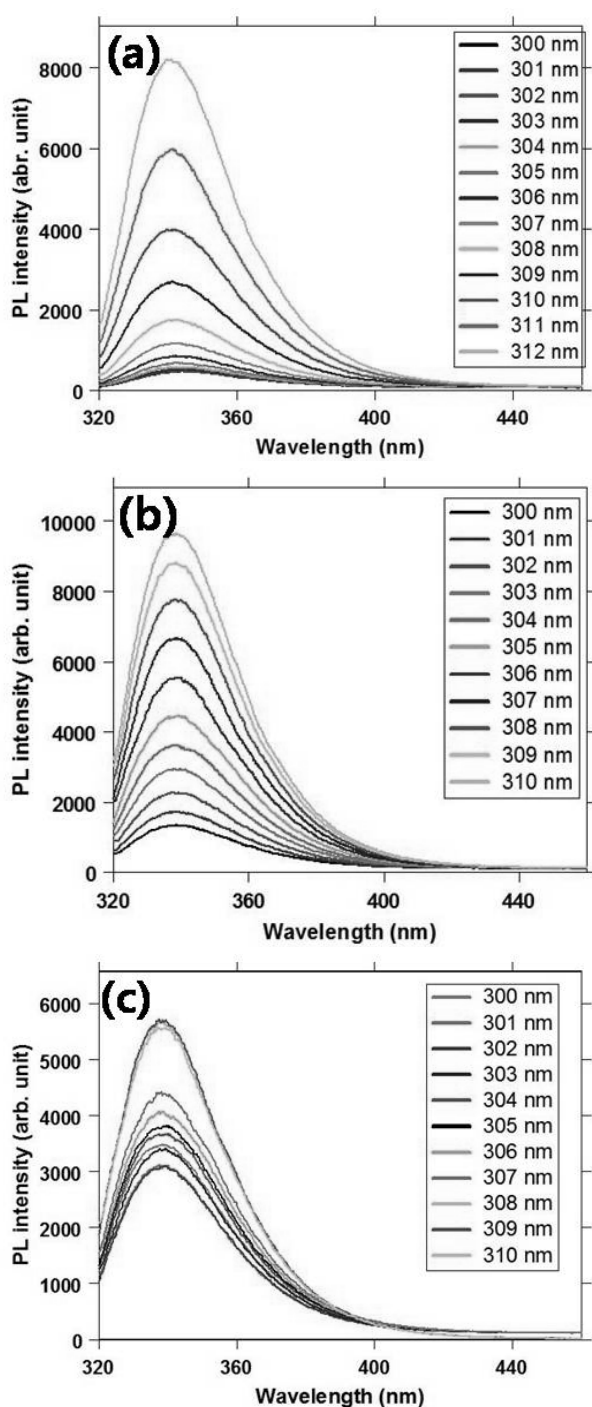


Fig. 4. PL spectra of (a) TiO₂An-A, (b) TiO₂PAn-B, (c) TiO₂An-C

synthetic processes is shown in Fig. 1. After addition acetic anhydride, no drastic color change was observed, which implied that polymerization of aniline moiety was not occurred.

FTIR spectra of TiO₂An-A, -B, and -C are compared in Fig. 2. The absorption peaks at around 3300 and 1669 cm⁻¹ are due to the -NH symmetric stretching and deformation, respectively. The absorption peaks at 3040, 1012, and 754 cm⁻¹ are caused by stretching, bending, and deformation of the aniline ring -CH,

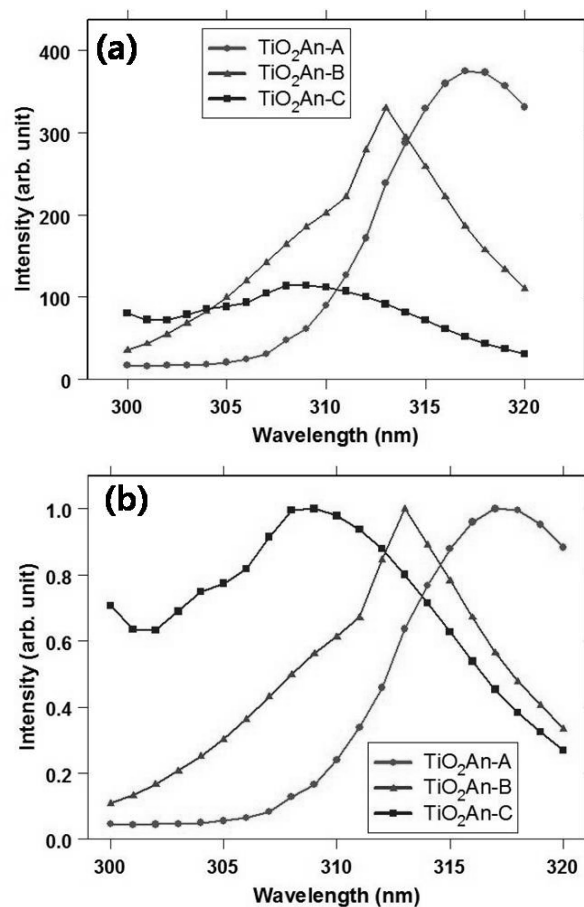


Fig. 5. Excitation wavelength dependent (a) PL intensity and (b) normalized the PL intensity

respectively. The aniline ring stretching peaks are appeared at 1600, 1548, and 1499 cm⁻¹. The absorption peak at 1442 cm⁻¹ represents the benzene ring -CH stretching vibration or -CH deformation. The absorption peaks at 1321 and 1265 cm⁻¹ represent the C-N stretching vibration. Absorption peak at 692 cm⁻¹ is due to the benzene ring bending vibration. The absorption peaks at 662, 613, and 504 cm⁻¹ appear from TiO₂ (13). The sequence of aniline related absorption intensities are TiO₂An-A, -B, and -C, which follow the sequence of the amount of aniline.

The colors of TiO₂An-A, -B, and -C are similar as shown in the picture in inset Fig. 3(a). However, the deep UV-range absorption increased with the increase of the amount of the aniline. The UV-visible absorption spectra with various amount of TiO₂An-A is shown in Fig. 3(b). The absorption intensity slightly increased with the increase of the amount of the TiO₂An-A. The similar results were obtained with the TiO₂-An-B and -C.

Excitation wavelength dependent PL spectra of TiO₂An-A, -B, and -C are shown in Fig. 4(a), 4(b), and 4(c), respectively. The emission peak was at 338 nm (3.69 eV) for all three

samples. For the TiO₂An-A, the emission intensity decreased and back up as the excitation wavelength increased until the excitation wavelength of 307 nm. Thereafter, the emission intensity exponentially increased with the increase of the excitation wavelength. For the TiO₂An-B, the luminescence intensity steadily increased with the increase the excitation wavelength as shown in Fig. 4(b). The emission intensity slowly increased until the excitation wavelength of 308 nm and decreased thereafter for the TiO₂An-C. Fig. 5(a) shows the integrated luminescence intensity. The emission intensity increased with the increase of the amount of aniline. Fig. 5(b) shows the normalized luminescence intensity, which exhibits the excitation wavelength of the maximum luminescence shifts toward longer wavelength with the increase the molar ration of the aniline.

4. Conclusions

Three different molar ratios of aniline and TiO₂ composite were synthesized with Ti(OPr)₄, aniline, and acetic anhydride. The characteristic infrared absorption peaks of aniline increased with the increase the molar ration of the aniline. The UV absorption slightly increased with increasing the amount of aniline ratio. The PL property was strongly dependent on the molar ratio of Ti(OPr)₄ and aniline, such as the luminescence intensities were exponentially increased with the increase the excitation wavelength from 307 to 317 nm, steadily increased from 300 to 313 nm and slowly increased from 302 to 308 nm for TiO₂An-A, -B, and -C, respectively, and decreased thereafter.

Acknowledgement

This work has been supported by Kyungil University in Korea.

References

1. Kumura M, Sakai R, Sato S, Fukawa T, Lkehara T, Maeda R, Mihara T. Sensing of vaporous organic compounds by TiO₂ porous films covered with polythiophene layers. *Advanced Functional Mater* 2012;22:469-76.
2. Borlaf M, Colomer MT, Moreno R, Andres A. Structural and photoluminescence study of Er³⁺/TiO₂ xerogels as a function of the temperature using optical techniques. 2015;98:338-45.
3. Edwards MOM, Persson R. A bistable viologen-TiO₂ color switch. *J Soc information display*. 2005;13:1035-37.
4. Singh P, Nanda A. Enhanced sun protection of nano-sized metal oxide particles over conventional metal oxide particles: An in vitro comparative study. *International J Cosmetic Sci* 2014; 36:273-83.
5. Parthiban S, Anuratha KS, Arunparabharan S, Abinesh S, Lakshminarasimhan N. Influence of GO incorporation in TiO₂ nanofibers on the electrode efficiency in dye-sensitized solar cells. *Ceramics Inter* 2015;41:1205-12.
6. Radhakrishnan S, Siju CR, Mahanta D, Patil S, Madras G. Conducting polyaniline-nano-TiO₂ composites for smart corrosion resistant coatings. *Electrochimica Acta* 2009;54:1249-54.
7. Xu H, Cao Q, Wang X, Li W, Li X, Deng H. Properties and chemical oxidation polymerization of pnyaniline/neutral red/TiO₂ composite electrodes. *Mater Sci Eng B* 2010;171:104-8.
8. Pawas SG, Sen CS, Patil VB. Development of nanostructured polyaniline-titanium dioxide gas sensors for ammonia recognition. *J Appl Polymer Sci* 2012;125:1418-24.
9. Li J, Zhao X, Zhang Z, Lai Y. Facile synthesis of hollow carbonized polyaniline spheres to encapsulate selenium for advanced rechargeable lithium-selenium batteries. *J Alloys and Compounds* 2015;619:794-99.
10. Bian C, Yu A, Wu H. Fibriform polyaniline/nano-TiO₂ composite as an electrode material for aqueous redox supercapacitors. *Electrochem Commun* 2009;11:266-9.
11. Gurunathan K, Amalnerkar DP, Trivedi DC. Synthesis and characterization of conducting polymer composite (PAN/TiO₂) for cathode material in rechargeable battery. *Mater Lett* 2003; 57:1642-8.
12. Fu X, Jia C, Wan Z, Weng X, Xie J, Deng L. Hybrid electrochromic film based on polyaniline and TiO₂ nanorods array. *Organic Electronics* 2014;15:2702-9.
13. Jin Y, Li G, Zhang Y, Zhang Y, Zhang L. Photoluminescence of anatase TiO₂ thin films achieved by the addition of ZnFe₂O₄. *J Phys: Condens. Matter*. 2001;13:L913.